

Musculoskeletal Pathology

# Genetically Augmenting A $\beta$ 42 Levels in Skeletal Muscle Exacerbates Inclusion Body Myositis-Like Pathology and Motor Deficits in Transgenic Mice

Masashi Kitazawa, Kim N. Green,  
Antonella Caccamo, and Frank M. LaFerla

*From the Department of Neurobiology and Behavior, Laboratory of Molecular Neuropathogenesis, University of California, Irvine, Irvine, California*

**The pathogenic basis of inclusion body myositis (IBM), the leading muscle degenerative disease afflicting the elderly, is unknown, although the histopathological features are remarkably similar to those observed in Alzheimer's disease. One leading hypothesis is that the buildup of amyloid- $\beta$  (A $\beta$ ) peptide within selective skeletal muscle fibers contributes to the degenerative phenotype. A $\beta$  is a small peptide derived via endoproteolysis of the amyloid precursor protein (APP). To determine the pathogenic effect of augmenting A $\beta$ 42 levels in skeletal muscle, we used a genetic approach to replace the endogenous wild-type presenilin-1 (PS1) allele with the PS1<sub>M146V</sub> allele in MCK-APP mice. Although APP transgene expression was unaltered, A $\beta$  levels, particularly A $\beta$ 42, were elevated in skeletal muscle of the double transgenic (MCK-APP/PS1) mice compared to the parental MCK-APP line. Elevated phospho-tau accumulation was found in the MCK-APP/PS1 mice, and the greater activation of GSK-3 $\beta$  and cdk5 were observed. Other IBM-like pathological features, such as inclusion bodies and inflammatory infiltrates, were more severe and prominent in the MCK-APP/PS1 mice. Motor coordination and balance were more adversely affected and manifested at an earlier age in the MCK-APP/PS1 mice. The data presented here provide experimental evidence that A $\beta$ 42 plays a proximal and critical role in the muscle degenerative process. (*Am J Pathol* 2006, 168:1986–1997; DOI: 10.2353/ajpath.2006.051232)**

Inclusion body myositis (IBM), the most prevalent muscle disorder among the elderly, is characterized by proximal and distal skeletal muscle weakness.<sup>1–3</sup> The clinical features of this disorder are characterized by muscle weak-

ness and atrophy, with selective involvement of both proximal and distal muscle groups, including the quadriceps, iliopsoas, triceps, and biceps muscles. In sporadic IBM, the majority of patients usually exhibit proximal weakness, and the quadriceps are more severely affected compared to other lower limb muscles.<sup>3</sup> In hereditary IBM, however, affected muscles may exhibit a more restricted focus. For example, the quadriceps may be selectively spared in certain autosomal recessive cases.<sup>4,5</sup> Histopathologically, both sporadic and hereditary IBM are characterized by atrophic muscle fibers and fibers containing rimmed vacuoles and abnormal protein aggregates, particularly amyloid- $\beta$  (A $\beta$ ), which is derived via endoproteolysis of the amyloid precursor protein (APP), and hyperphosphorylated tau.<sup>2,6–10</sup>

IBM and Alzheimer's disease (AD) share many pathohistological features including the buildup of aggregated proteins such as A $\beta$  and tau. In this regard, IBM can also be considered as a proteinopathy. As in AD, the role of the A $\beta$  peptide is unresolved, although evidence suggests that it plays an early and critical role in the muscle degeneration. IBM remains the only known condition in which A $\beta$  accumulates pathologically outside the central nervous system, except for age-related macular degeneration.<sup>11</sup> This distinction implicates a critical role for A $\beta$  in the pathogenesis of IBM. A noteworthy difference between two degenerative processes is the location in which A $\beta$  accumulates. In AD, A $\beta$  has been traditionally viewed to exert its pathological effects extracellularly where it builds up in amyloid plaques, whereas it is only found intracellularly in IBM.<sup>12</sup> However, recent studies have demonstrated that various assembly states of A $\beta$  found intracellularly contribute to pathophysiological changes in AD as well, including our own studies in transgenic mice in which intraneuronal A $\beta$  appears to induce deficits in synaptic plasticity and trigger the onset of cognitive decline.<sup>13,14</sup> Moreover, soluble oligomeric

Supported by the National Institutes of Health (grant AG 20335).

Accepted for publication February 28, 2006.

Address reprint requests to Frank M. LaFerla, Ph.D., Department of Neurobiology and Behavior, 1109 Gillespie Neuroscience Facility, University of California, Irvine, Irvine, CA 92697-4545. E-mail: laferla@uci.edu.

A $\beta$  is now considered to be a potent neurotoxic component, found in the AD brain, and the levels of A $\beta$  oligomers in brain, unlike fibrillar A $\beta$  levels, correlates well with cognitive decline.<sup>15-18</sup> It is important to note that there is evidence that this species of A $\beta$  occurs intraneuronally.<sup>19,20</sup> Taken together, these data suggest a critical pathogenic role for intracellular A $\beta$  in AD.

We previously developed a transgenic model of IBM by overexpressing the human Swedish APP mutation in skeletal muscle under the control of the *muscle creatine kinase (MCK)* promoter.<sup>21</sup> These mice generate A $\beta$ , although the predominant isoform is the less amyloidogenic A $\beta$ 40 peptide. Although A $\beta$ 42 is considered more pathogenic in AD, it remains unclear whether it is more pathogenic in skeletal muscle compared to A $\beta$ 40. Here we used a genetic approach to selectively increase A $\beta$ 42 levels. Mutations in the *presenilin-1 (PS1)* gene associated with familial AD (FAD) are well known to modulate  $\gamma$ -secretase function to selectively increase the formation of the more amyloidogenic A $\beta$ 42 peptide in neurons.<sup>22,23</sup> Notably, this effect is not limited to neurons because FAD mutations in PS1 are also known to significantly augment A $\beta$ 42 levels in various cell culture models and transgenic animals.<sup>22,24,25</sup> We report that MCK-APP mice harboring the PS1<sub>M146V</sub> knock-in mutation (MCK-APP/PS1) produce markedly higher levels of A $\beta$ 42 than the parental MCK-APP mice. The double transgenic mice develop histopathological features resembling IBM, including centric nuclei, intracellular accumulation of A $\beta$  peptide, and enhanced inflammation around affected muscle fibers. Notably, elevated A $\beta$ 42 levels further lead to increased phosphorylation of tau in skeletal muscle. We also find that enzymatic activity for cyclin-dependent kinase 5 (cdk5) and glycogen synthase kinase 3 $\beta$  (GSK-3 $\beta$ ) are elevated. These pathophysiological changes lead to an earlier onset of motor deficits in the MCK-APP/PS1 mice. These results implicate an integral role for A $\beta$ 42 in the progression of muscle degeneration, and suggest that A $\beta$ -directed therapies may be effective for the treatment of human IBM patients.

## Materials and Methods

### Generation of Double Transgenic Mice

Hemizygous MCK-APP mice (of the A6 line) were crossed to homozygous PS1<sub>M146V</sub> knock-in (PS1-KI) mice to generate F<sub>1</sub> offspring.<sup>21,26</sup> PS1-KI mice, maintained on a C57BL/6 background like the MCK-APP transgenic mice, are homozygous for the mutant PS1<sub>M146V</sub> allele. Because the mutation was knocked-in, expression of the mutant PS1 protein is under the transcriptional control of the endogenous promoter, thereby ensuring expression in skeletal muscle.

For biochemical analyses, skeletal muscle tissues from nontransgenic (wild-type C57BL/6 background: non-Tg), PS1-KI, single transgenic MCK-APP, and double transgenic MCK-APP/PS1 mice were homogenized in T-PER extraction buffer (Pierce, Rockford, IL) in the presence of protease inhibitor cocktail (Roche Applied Science, Indi-

anapolis, IN) and phosphatase inhibitors (5 mmol/L sodium fluoride and 50  $\mu$ mol/L sodium orthovanadate). The detergent-soluble fraction was isolated by centrifugation at 100,000  $\times g$  for 1 hour at 4°C. The resultant pellet was homogenized in 70% formic acid followed by centrifugation at 100,000  $\times g$  for 1 hour at 4°C to isolate the detergent-insoluble fraction.

### Expression Analysis

Calf muscles, quadriceps, and triceps were dissected from 4-month-old MCK-APP/PS1 double transgenic mice and controls (PS1-KI), and total RNA was isolated using TRI reagent (Molecular Research Center, Cincinnati, OH). To determine levels of human APP expression, isolated RNA (10  $\mu$ g) was analyzed by Northern blot using <sup>32</sup>P-labeled 0.24-kb simian virus 40 (SV40) poly(A) DNA fragment as described previously.<sup>21</sup> Briefly, the human APP transgene was constructed with the use of the MCK promoter so that gene expression would be targeted to skeletal muscle. The transgene also included the polyadenylation signal from SV40. Because the SV40 sequence is not present in PS1-KI mice, this sequence can serve as a specific probe to detect the human APP transgene mRNA product selectively in the transgenic mice. Equal RNA loading was confirmed by probing for GAPDH (Ambion, Austin, TX).

### Immunohistochemical Analysis

Skeletal muscle tissue was snap-frozen in liquid nitrogen-cooled isopentane and stored at -80°C. Cryosections were cut at 10  $\mu$ m, placed onto silane-coated slides, and stored at -20°C. Hematoxylin and eosin staining was performed to determine the general morphology of the muscle. Serial sections were immunostained to determine the localization of APP and A $\beta$  fragments. Mouse anti-human A $\beta$  antibody 6E10 (Signet, Dedham, MA) was used to stain both human APP and A $\beta$ -containing fragments, P2-1 antibody recognizes full-length human APP (gift from Dr. William Van Nostrand, State University of New York at Stony Brook), and anti-mouse CD8 antibody (Serotec, Raleigh, NC) was used to detect activated inflammatory T cells.

### Immunoprecipitation

Immunoprecipitation was performed before the kinase assay. One hundred  $\mu$ g of skeletal muscles from 6- and 14-month-old PS1-KI or MCK-APP/PS1 mice were immunoprecipitated with protein A-agarose (Calbiochem, La Jolla, CA) for cdk5 antibody or protein G-agarose (Roche Applied Science) for GSK-3 $\beta$  or AT8 antibodies overnight at 4°C. The resultant protein-antibody-agarose complex was washed three times with 0.5 $\times$  STEN (25 mmol/L Tris, pH 7.6, 75 mmol/L NaCl, 1 mmol/L ethylenediaminetetraacetic acid, and 0.1% Nonidet P-40). For immunoblotting, the complex was then resuspended in 2 $\times$  loading buffer and incubated for 10 minutes at 70°C.

### Immunoblot Analysis

Equal amounts of protein from each fraction were resolved by sodium dodecyl sulfate-polyacrylamide gel electrophoresis (4 to 12% Bis-Tris gel from Invitrogen, Carlsbad, CA). After transfer onto nitrocellulose, the blots were incubated with the respective antibodies: 6E10 (1:1000); anti-C-terminal fragment of APP (1:5000; Cell Signaling Technology, Beverly, MA); anti-PS1 (1:500, Cell Signaling Technology); AT8 (phosphorylated tau at serine 202 and threonine 205; 1:2000; Innogenetics, Alpharetta, GA); anti-cdk5 (1:1000, Calbiochem); anti-GSK-3 $\beta$  (1:1000; BD Transduction Laboratories, San Diego, CA); anti-GSK-3 $\beta$  (phosphorylated at serine 9, 1:1000; Cell Signaling Technology), anti-p38 MAPK (1:1000, Cell Signaling Technology), anti-phospho-p38 MAPK (phosphorylated at threonine 180 and tyrosine 182, 1:1000; Cell Signaling Technology), anti-JNK (1:1000; Cell Signaling Technology), and anti-phospho-JNK (phosphorylated at threonine 183 and tyrosine 185, 1:1000; Cell Signaling Technology) followed by horseradish peroxidase-conjugated secondary antibodies. Protein bands were detected by enhanced chemiluminescence plus (Amersham Biosciences, Piscataway, NJ). Membranes were reprobbed with antibody against GAPDH (1:5000; Santa Cruz Biotechnology, Santa Cruz, CA) to control for protein loading.

### Enzyme-Linked Immunosorbent Assay (ELISA) $A\beta$ Measurement

Both detergent-soluble and -insoluble fractions were used to detect  $A\beta$ 40 and  $A\beta$ 42 by ELISA as described previously.<sup>14,21,27</sup> MaxiSorp immunoplates (Nalge Nunc, Rochester, NY) were coated with antibody against  $A\beta$ 1-17 (gift from Dr. William Van Nostrand) at a concentration of 25  $\mu\text{g}/\mu\text{l}$ , and  $A\beta$ 40 and  $A\beta$ 42 were detected by specific horseradish peroxidase-conjugated antibody against  $A\beta$ 35-40 (MM32-13.1.1) or  $A\beta$ 35-42 (MM40-21.3.4), respectively.

### GSK-3 $\beta$ and cdk5 Kinase Assays

Kinase assays were performed as described previously.<sup>27</sup> Briefly, after immunoprecipitation with GSK-3 $\beta$  or cdk5 antibodies, samples were mixed with 50  $\mu\text{l}$  of reaction mixture containing 20 mmol/L MOPS, pH 7.2, 5 mmol/L  $\text{MgCl}_2$ , 1 mmol/L sodium orthovanadate, 5 mmol/L NaF, 100  $\mu\text{mol/L}$  ATP, 2.5  $\mu\text{Ci}$  [ $\gamma$ -<sup>32</sup>P]ATP, and 0.2 mmol/L cdk5 substrate (Calbiochem) or 0.2 mmol/L GSK-3 $\beta$  substrate (Calbiochem). The reaction transpired for 1 hour at 37°C, then 35  $\mu\text{l}$  of supernatant was placed on Immobilon-nitrocellulose membrane (Millipore, Billerica, MA). The membranes were washed in 0.3% phosphoric acid and counted in a scintillation counter to determine the kinase activity.

### Isolation of mRNA and Quantification of Inflammation by Real-Time Polymerase Chain Reaction (RT-PCR)

Total RNA was isolated from quadriceps of non-Tg, PS1-KI, MCK-APP, and MCK-APP/PS1 mice (14 and 24 months old) using TRI reagent (Molecular Research Center), and cDNA was synthesized using iScript cDNA synthesis kit (Bio-Rad Laboratories, Hercules, CA) as described previously.<sup>27</sup> Equal amounts of cDNA (~1  $\mu\text{g}$ ) were subject to RT-PCR reaction for mouse CD8 mRNA by iQ SYBR Green supermix (Bio-Rad Laboratories) using primer pair of 5'-TGT GAA GCC AGA GGA CAG TG-3' and 5'-CAG GAT GCA GAC TAC CAG CA-3'. Cycle threshold (Ct) values were calculated by MyiQ software (Bio-Rad Laboratories), and the relative fold changes in mRNA were determined as relative to GAPDH mRNA levels in each treatment group (mouse GAPDH primer pair: 5'-AAC TTT GGC ATT GTG GAA GG-3' and 5'-ACA CAT TGG GGG TAG GAA CA-3').

### Rotarod Motor Test

Motor performance was evaluated using the accelerating rotarod (Accuscan Instruments, Columbus, OH) as described previously.<sup>21</sup> Mice were placed on a rotating dowel and required to continuously walk forward to avoid falling off. The rod was accelerated throughout 20 seconds to a constant speed of 10 rpm, and each trial was ended at 60 seconds. Non-Tg, PS1-KI, MCK-APP, and MCK-APP/PS1 mice (ages 1 to 23 months) were given 10 training trials per day for 2 consecutive days, and probe trials were completed on the third day. In the probe trial, each mouse was tested five times and time of fall-off was recorded and averaged.

### Statistical Analysis

All data were analyzed using one-way analysis of variance or unpaired *t*-test, and *P* < 0.05 or lower was considered to be significant.

## Results

### Introduction of PS1<sub>M146V</sub> Allele Does Not Alter Transgene Expression and Steady-State Levels

To test the phenotypic consequences of augmenting  $A\beta$ 42 levels in skeletal muscle, we used a genetic approach to introduce a mutant PS1 allele into the MCK-APP single transgenic line by crossing them to homozygous PS1-KI mice. Double transgenic mice, referred to as MCK-APP/PS1 mice consisted of the following genotype: homozygous for the PS1<sub>M146V</sub> allele and hemizygous for the MCK-APP transgene. It was first necessary to determine whether the expression profile of the MCK-APP transgene was altered in the MCK-APP/PS1 mice. We analyzed total mRNA from various tissues by Northern blot and found that, as in the parental MCK-APP trans-

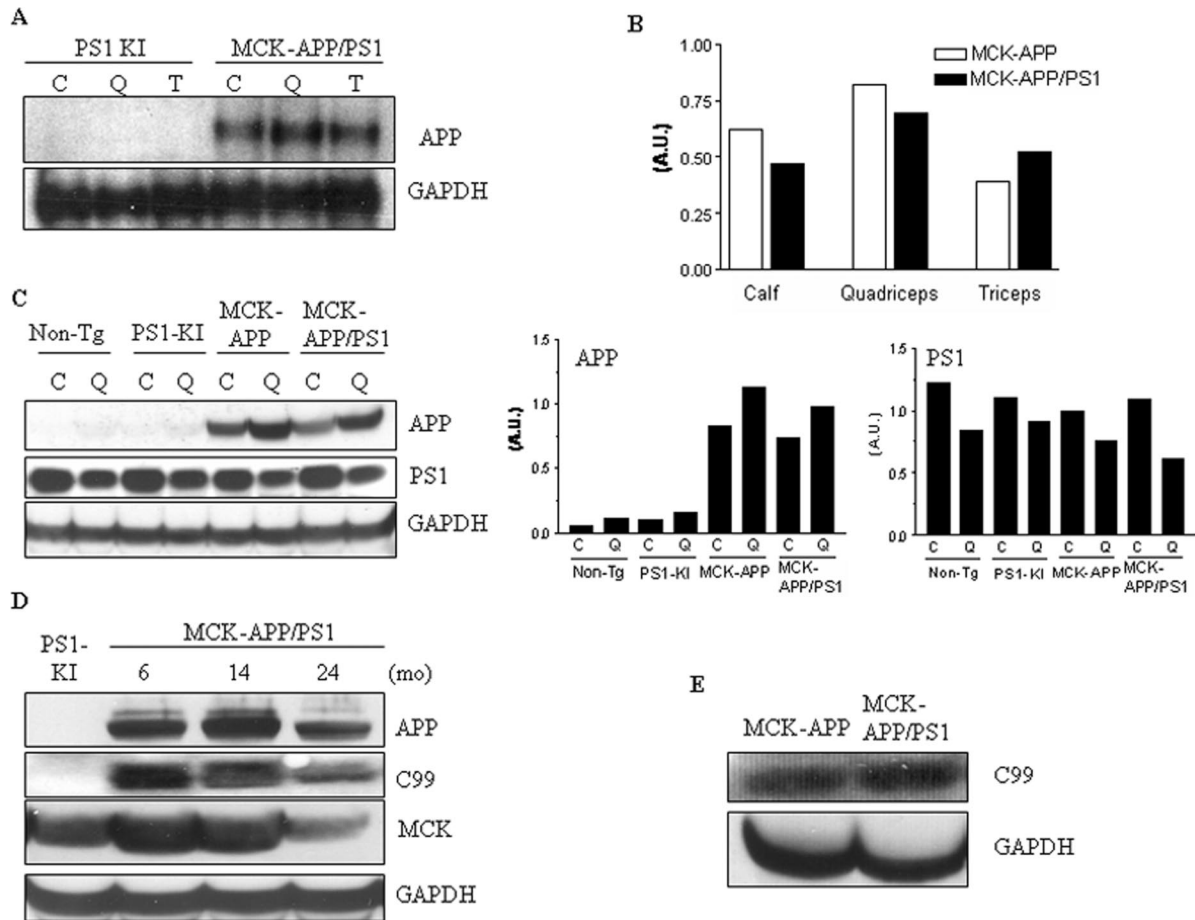


**Figure 1.** Expression of the transgene and steady-state levels of APP and PS1 in skeletal muscle is not altered between MCK-APP and MCK-APP/PS1 transgenic mice. **A:** Northern blot analysis of human *APP* transgene mRNA from calf muscle (C), quadriceps (Q), and triceps (T), of PS1-KI and MCK-APP/PS1 mice reveals the human *APP* transgene is only expressed in MCK-APP/PS1 mice. Quadriceps has the highest transgene expression levels among other muscles. **B:** Densitometric comparison of the level of human *APP* transgene expression between the single transgenic MCK-APP mice and double transgenic MCK-APP/PS1 mice. Graph represents densitometric analysis of human mRNA band. No overall difference in the expression level is apparent, indicating that PS1-KI allele does not alter expression of the *MCK-APP* transgene in the MCK-APP/PS1 mice. **C:** Immunoblotting of transgene products from calf muscle (C) and quadriceps (Q) of nontransgenic (non-Tg), PS1-KI, MCK-APP, and MCK-APP/PS1 mice shows that the steady-state levels of APP detected by 6E10 antibody is present in MCK-APP and MCK-APP/PS1 mice but not in non-Tg or PS1-KI. Membranes were reprobed for GAPDH as a loading control. Graphs represent the intensity of APP (**left**) and PS1 (**right**) in the immunoblotting. **D:** Age-dependent change in APP steady-state levels in the MCK-APP/PS1 mice. Quadriceps from 6-, 14-, and 24-month-old MCK-APP/PS1 mice shows highest APP levels at 14 months, and lower levels at 24 months. C99 levels were highest at 6 to 14 months and also decreased with age. MCK levels showed a similar trend, indicating that the reduction in APP steady-state levels is attributable to the decreased activity of the MCK promoter. Membranes were reprobed for GAPDH to control for equal loading. **E:** The steady-state levels of C99 between the MCK-APP and MCK-APP/PS1 mice at 14 months of age. No apparent difference was detected in the C99 levels, indicating no alteration of BACE cleavage by introduction of PS1 mutation.

genic line,<sup>21</sup> expression of the human *APP* transgene was exclusively directed to muscle tissue (data not shown). We next compared the expression levels of APP in various skeletal muscles of the double transgenic MCK-APP/PS1 mice to the same muscles from the parental PS1-KI or MCK-APP mice. As expected, human APP mRNA is only apparent in the double transgenic mice and not in the PS1-KI mice (Figure 1A). Likewise, the levels of the transgene transcript are comparable between the MCK-APP and MCK-APP/PS1 mice, suggesting that the introduction of the *PS1*<sub>M146V</sub> mutation did not alter the expression pattern or levels of the human *APP* transgene (Figure 1B).

We next determined the effect of introducing the *PS1*<sub>M146V</sub> knockin mutation on human APP steady-state levels in skeletal muscle. Notably, human APP steady-state levels were comparable between both mouse groups, indicating that the introduction of the mutant *PS1*

gene did not alter the steady-state levels of the human APP protein (Figure 1C). As expected, no signal was detected in muscle from non-Tg and PS1-KI mice after probing with the human-specific APP antibody (Figure 1C). The levels of PS1 in skeletal muscle were also examined and compared by Western blotting among the non-Tg, PS1-KI, MCK-APP, and MCK-APP/PS1 mice and revealed that there was no difference in the steady-state levels among the four mouse groups, indicating that the *PS1*<sub>M146V</sub> mutant protein was maintained at physiological levels and not altered by the *MCK-APP* transgene (Figure 1C).

We next determined whether the steady-state levels of the human APP protein changed as a function of age. We compared three ages: 6, 14, and 24 months of age. Interestingly, the steady-state levels of the holoprotein as well as its proteolytic fragment C99 differed as the mice aged. The highest level of holoprotein was detected at

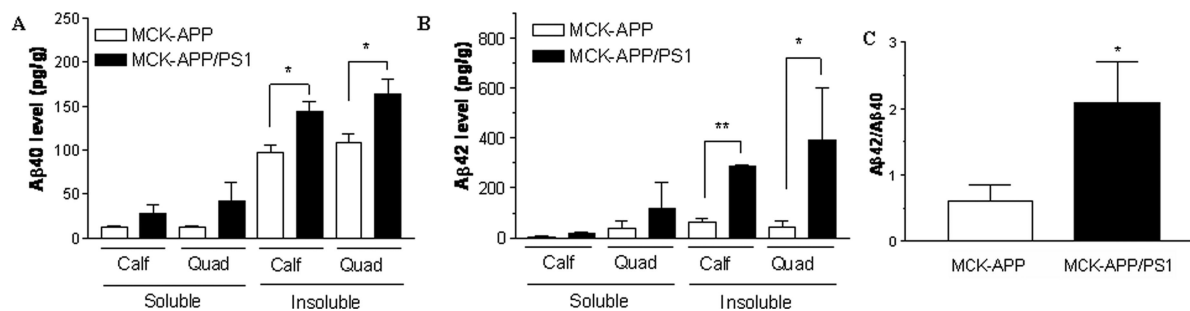


**Figure 2.** Augmenting Aβ42 production in skeletal muscle of MCK-APP/PS1 mice. **A** and **B**: Both detergent-soluble and -insoluble fractions from calf muscle and quadriceps of 14- to 15-month-old MCK-APP (open bars) or MCK-APP/PS1 (filled bars) mice were used to measure total Aβ40 and Aβ42 by ELISA using specific antibodies against Aβ35-40 (MM32-13.1.1) and Aβ35-42 (MM40-21.3.4), respectively. Significant ( $P < 0.05$  or less) increases in Aβ40 and Aβ42 were detected in skeletal muscle from MCK-APP/PS1 mice. \* $P < 0.05$  or \*\* $P < 0.01$  as compared between MCK-APP and MCK-APP/PS1 mice. Number of mice used:  $n = 6$  (MCK-APP) and  $n = 7$  (MCK-APP/PS1). **C**: The Aβ42/Aβ40 ratio significantly increases in MCK-APP/PS1 mice as compared to MCK-APP mice at 14 months of age. \* $P < 0.05$ .

~14 months of age, and was markedly lower in skeletal muscle from 24-month-old mice (Figure 1D). This pattern was consistent with our previous finding in the single MCK-APP line.<sup>21</sup> This age-related decrease in transgene levels appears to be attributable to an age-associated decline in the activity of the *MCK* promoter, as we find that the steady-state levels of the endogenous mouse *MCK* protein are also markedly decreased at 24 months (Figure 1D). Compared to the age-matched parental MCK-APP mice, C99 levels were slightly increased in the MCK-APP/PS1 mice at 14 months of age although the difference did not achieve statistical significance (Figure 1E). Therefore, because the pattern and levels of the human APP transgene were not modulated by the introduction of PS1<sub>M146V</sub> gene, and the levels of PS1 protein were also maintained at physiological levels, any change in the onset of the phenotype must be due to modulating APP processing to favor Aβ42 formation.

### Augmenting Aβ42 Exacerbates the IBM-Like Pathology in Skeletal Muscle of the MCK-APP/PS1 Transgenic Mice

A key question to resolve is whether the processing of the APP protein in skeletal muscle is altered in response to the introduction of the *PS1* mutation and to determine which Aβ species, Aβ40 or Aβ42, predominates. In our previous study, both Aβ40 and Aβ42 were produced in skeletal muscle of the parental MCK-APP transgenic mice based on SELDI-MS analysis, although it was clear that Aβ40 levels were much higher than Aβ42 levels.<sup>28</sup> This observation confirms that both Aβ40 and Aβ42 are produced in skeletal muscle of the MCK-APP mice and that these levels are markedly higher than those in age-matched non-Tg mice.<sup>28</sup> Because the goal of this current study was to specifically augment Aβ42 levels, we next quantitatively determined the levels of both Aβ species in muscles of the MCK-APP/PS1 mice by ELISA using end-specific antibodies against Aβ40 and Aβ42. Protein extracts were prepared from the quadriceps and calf muscle of 14-month-old non-Tg, PS1-KI control, MCK-APP, and MCK-APP/PS1 mice. No detectable Aβ40 or Aβ42 was found in muscle from non-Tg or PS1-KI mice (data

not shown), whereas relatively high levels of detergent-insoluble Aβ40 and Aβ42 were detected in muscle from the MCK-APP/PS1 mice (Figure 2, A and B). Furthermore, the ratio of Aβ42/Aβ40 was markedly elevated in the MCK-APP/PS1 mice compared to the parental MCK-APP mice (Figure 2C). Therefore, as in neurons, the introduction of the *PS1* mutation in muscle shifted the processing of APP to favor the generation of Aβ42 and also increased total Aβ production.

We further examined the age-dependent processing of APP in the MCK-APP/PS1 mice. Both calf muscle and quadriceps were harvested from MCK-APP/PS1 mice at 3, 6, 14, and 24 months of age, and detergent-soluble Aβ40 and Aβ42 were measured. The levels of Aβ40 and Aβ42 in calf muscles and quadriceps increased in an age-dependent manner up to 14 months of age but were lower at 24 months (data not shown). This change corresponded to the lower APP steady-state levels that were observed at 24 months of age (Figure 1D).

Having demonstrated that the introduction of the mutant *PS1* allele into the MCK-APP mice augments Aβ42 levels, we next histopathologically evaluated the double MCK-APP/PS1 transgenic mice using several criteria. First, we compared muscle sections from aged mice stained with the general stain hematoxylin and eosin and compared results to the parental PS1-KI and MCK-APP transgenic lines. No alterations in muscle cytoarchitecture were apparent in PS1-KI mice and the muscle appeared normal with peripherally localized nuclei and intact smooth muscle linings even in mice as old as 24 months of age (Figure 3, A and B). In contrast, muscle (calf and quadriceps) from MCK-APP/PS1 mice exhibited abundant centric nuclei (Figure 3, C and D). A similar histological feature was also observed in age-matched MCK-APP mice muscle (Figure 3I). Centric nuclei are a general marker of muscle pathology often observed in muscle disorders, although they can occasionally be found in normal mouse and human tissue at a low frequency of ~1 to 3%; centric nuclei are also a feature of IBM myopathology.<sup>29</sup> In addition, histological analysis revealed that a significant proportion of the muscle fibers in the MCK-APP/PS1 mice were smaller in size compared to control mice. These affected muscle cells were sur-

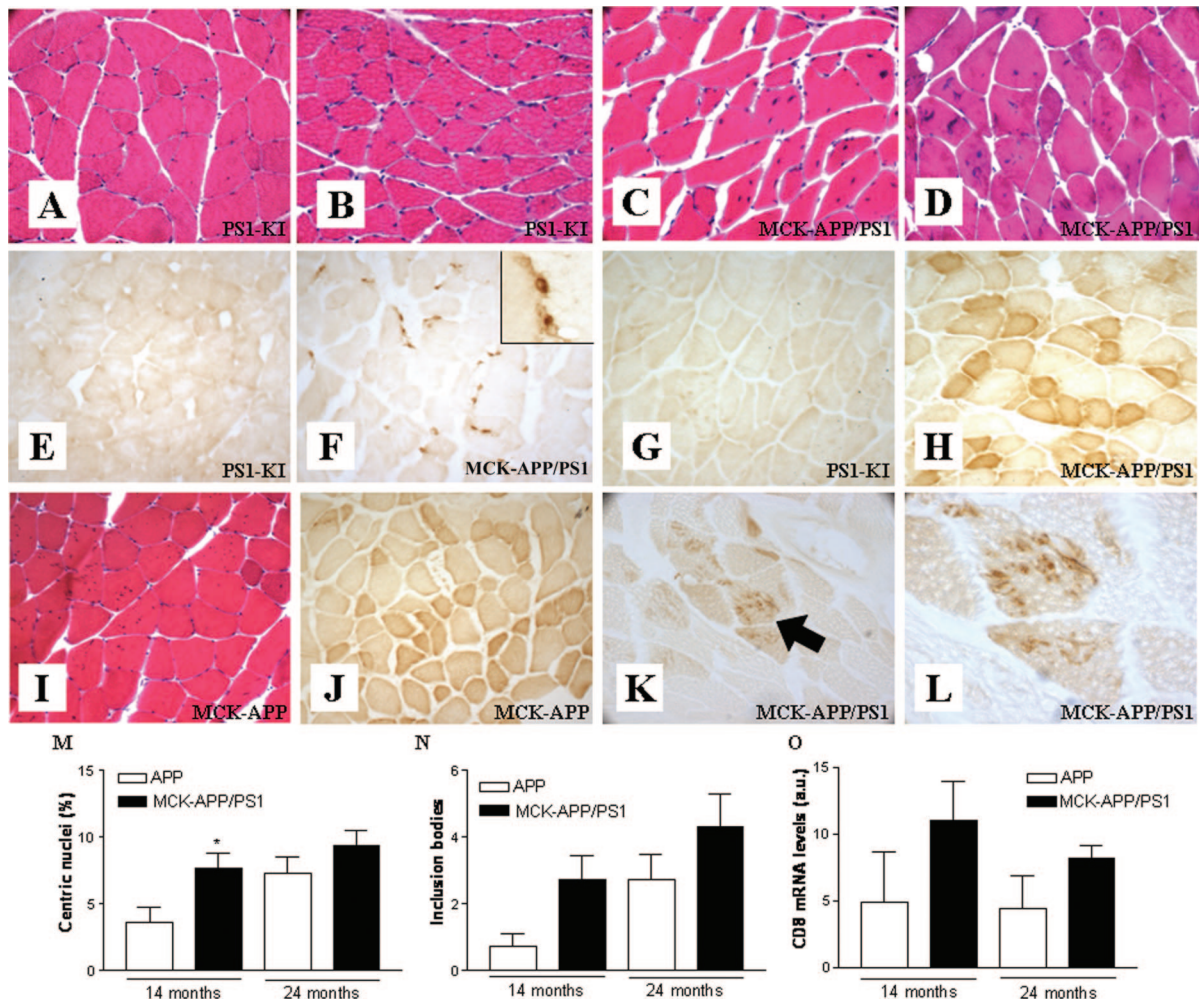


**Figure 3.** IBM-like histopathological hallmarks are evident in skeletal muscle from the MCK-APP/PS1 mice. H&E staining of calf muscle (A) and quadriceps (B) from 24-month-old PS1-KI or calf muscle (C) and quadriceps (D) of 24-month-old MCK-APP/PS1 mice. E and F: CD8 immunostaining of quadriceps from 24-month-old PS1-KI mice and MCK-APP/PS1 mice. F: Skeletal muscle from MCK-APP/PS1 mice exhibits increased numbers of CD8-positive activated T cells around muscle fibers. Inset is a higher magnification view of CD8-positive T cells. G: Full-length human APP immunostaining (P2-1) of quadriceps muscle from 24-month-old PS1-KI. H: P2-1 immunostaining of quadriceps from 24-month-old MCK-APP/PS1, confirming the presence of APP in muscle fibers, and APP-immunopositive fibers tend to be smaller in size compared to nonstained fibers. I and J: Calf muscle from 24-month-old MCK-APP mice was stained with H&E (I) or P2-1 antibody (J) for comparison with MCK-APP/PS1 mice. The histopathological staining shows similar histopathological patterns with MCK-APP/PS1 mice shown above. K: Intracellular A $\beta$  staining in quadriceps of MCK-APP/PS1 mice, and at higher magnification (L). M: The percentage of centric nuclei-containing muscle fibers in the parental MCK-APP and MCK-APP/PS1 mice at 14 or 24 months of age. The graph represents mean  $\pm$  SEM of seven animals per group. N: The number of A $\beta$ -containing inclusions in the parental MCK-APP and MCK-APP/PS1 mice at 14 or 24 months of age. Muscle sections were immunostained with 6E10 antibody, and intracellular A $\beta$  inclusions were counted in random field. The graph represents mean  $\pm$  SEM of seven animals per group. O: RT-PCR for CD8 mRNA levels in quadriceps of MCK-APP or MCK-APP/PS1 mice. The expression levels were individually normalized by GAPDH mRNA levels. The graph represents relative CD8 mRNA levels to age-matched non-Tg or PS1-KI mice. There was no significant difference between non-Tg and PS1-KI mice.

rounded by a relatively large number of hematoxylin-positive nuclei, most likely inflammatory cells.

Another major pathological hallmark of IBM is immune infiltration. Consequently, we analyzed and compared muscle tissue from MCK-APP/PS1 mice to age-matched PS1-KI mice (Figure 3E). We observed extensive numbers of CD8-immunopositive T cells surrounding or infiltrated into muscle fibers from the MCK-APP/PS1 mice (Figure 3F). Thus, whereas the single MCK-APP line showed neutrophil rather than T-cell infiltration,<sup>21</sup> by augmenting A $\beta$ 42 levels in skeletal muscle of the MCK-APP/PS1 mice, we have derived a model that better mimics the inflammatory response of human IBM by inducing T-cell infiltration.

Using immunohistochemistry, we showed that human APP was readily apparent in skeletal muscle using antibody P2-1 antibody. In contrast, no staining was observed in muscles from the PS1-KI mice (Figure 3G). Both MCK-APP and MCK-APP/PS1 mice showed high levels of P2-1-immunopositive muscle fibers (Figure 3, H and J), confirming the buildup of the transgene product in certain muscle fibers. The numbers of P2-1-immunopositive muscle fibers were comparable between the two transgenic mice. As a rule, these P2-1-immunoreactive fibers were relatively smaller in size compared to other nonreactive muscle cells.

Inclusion bodies are the defining hallmark feature of IBM and are believed to play an important pathogenic

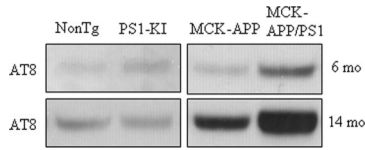


**Figure 4.** Tau phosphorylation is elevated in skeletal muscle of MCK-APP/PS1 mice. The steady-state levels of phosphorylated tau were examined using antibody AT8. Tau-immunoreactive band from calf muscles of 6- or 14-month-old non-Tg, PS1-KI, MCK-APP, and MCK-APP/PS1 mice are shown. Data are representative of four mice per group per age, and membranes were reprobbed for GAPDH to control for equal loading (data not shown).

role in muscle degeneration. ELISA data showed that A $\beta$ 42 was predominantly produced in the skeletal muscle of the MCK-APP/PS1 mice (Figure 2, A–C). We immunostained muscle with A $\beta$ -specific antibodies and observed prominent accumulation of A $\beta$  intracellularly. Quadriceps from aged MCK-APP/PS1 mice showed numerous intracellular inclusions that were immunoreactive with the A $\beta$ -specific antibodies (Figure 3, K and L), indicating that the MCK-APP/PS1 mice mimic this important pathological feature of human IBM.

We next quantitatively measured pathological hallmarks of IBM including centric nuclei, A $\beta$  inclusion bodies, and inflammatory responses between the MCK-APP and MCK-APP/PS1 mice at 14 and 24 months of age.

Numbers of centric nuclei were markedly higher in skeletal muscle of MCK-APP/PS1 at 14 months compared to age-matched parental MCK-APP mice ( $P < 0.05$ ; Figure 3M). By the age of 24 months, the relative percentage of centric nuclei-containing cells was not different between the two mouse groups (Figure 3M). Similarly, the number of A $\beta$ -containing inclusion bodies was greater in the MCK-APP/PS1 mice than the parental MCK-APP mice (Figure 3N). Furthermore, we noted that inflammation, as determined by CD8 mRNA expression, in skeletal muscle occurred earlier in the MCK-APP/PS1 mice compared to the parental line. CD8 mRNA levels increased approximately two times in 14-month-old MCK-APP/PS1 mice compared to the MCK-APP mice (Figure 3O). Taken together, these results show that augmenting A $\beta$ 42 exacerbates the IBM-like muscle pathology in the double transgenic mouse model.

### Enhanced GSK-3 $\beta$ and cdk5 Activity in Skeletal Muscle of the MCK-APP/PS1 Mice

Hyperphosphorylation of tau and subsequent accumulation of tau tangles in skeletal muscles are a major pathological hallmark of IBM. We examined whether tau phosphorylation was affected by the exacerbation of the

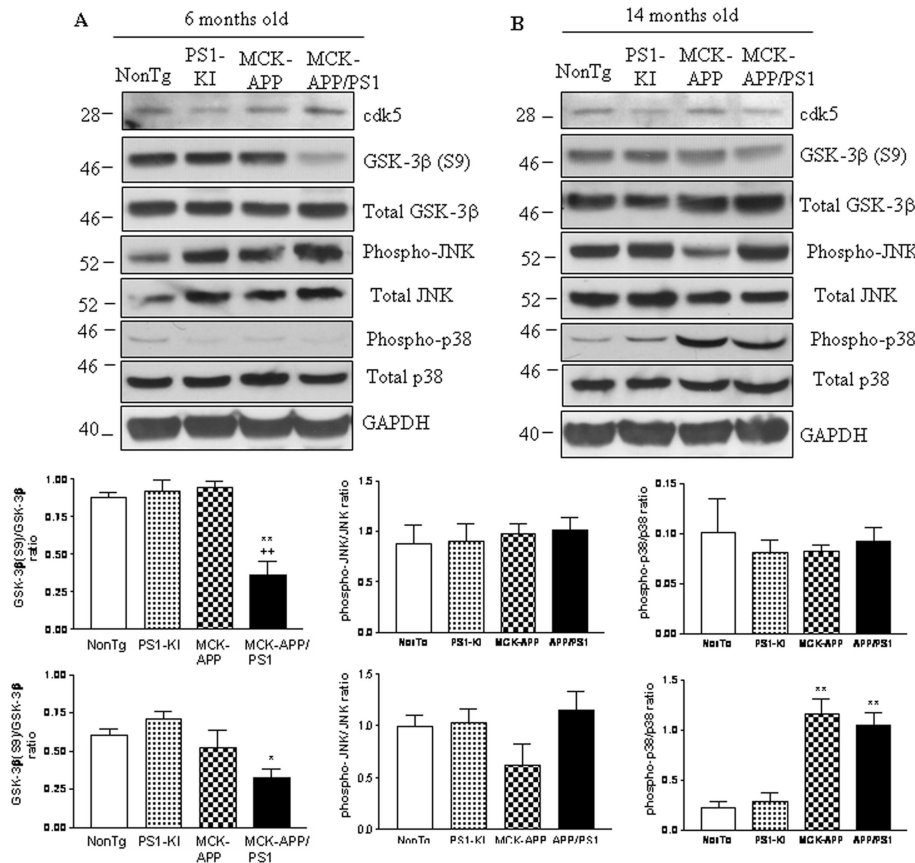


**Figure 5.** Increased tau phosphorylation in skeletal muscle of MCK-APP/PS1 mice is mediated by GSK-3 $\beta$  and cdk5. Steady-state levels of JNK, p38-MAPK, cdk5, GSK-3 $\beta$ , and their phosphorylated states were examined from 6- (A) and 14-month-old mice (B). Specifically, we determined whether each kinase was phosphorylated at selective residues known to affect their activity: threonine 183 and tyrosine 185 for JNK, threonine 180 and tyrosine 182 for p38-MAPK, and serine 9 for GSK-3 $\beta$ . The graphs represent ratio of the intensity of phosphorylated state relative to total level of corresponding kinase. \* $P < 0.05$  or \*\* $P < 0.01$  compared to non-Tg and PS1-KI, and  $^{++}P < 0.01$  compared to MCK-APP.

amyloid pathology in skeletal muscle at 6 and 14 months of age. No shift in the AT8-positive tau (phosphorylated at serine 202 and threonine 205; S202/T205) band was apparent in either non-Tg or PS1-KI mice at all ages tested, indicating that the PS1<sub>M146V</sub> mutation alone did not alter the tau phosphorylation pattern (Figure 4). Notably, we found that the levels of AT8-positive tau were increased in the MCK-APP/PS1 mice compared to the MCK-APP mice (Figure 4). The difference in phosphorylated tau levels between the MCK-APP and the MCK-APP/PS1 mice was even more apparent at 14 months of age, where approximately fourfold more phosphorylated (AT8-positive) tau was observed in the MCK-APP/PS1 mice (Figure 4).

Several kinases including c-Jun N-terminal kinase (JNK), p38 mitogen-activated protein kinase (p38-MAPK), cyclin-dependent kinase 5 (cdk5), and glycogen synthase kinase-3 $\beta$  (GSK-3 $\beta$ ), have been extensively evaluated for their role in the phosphorylation of tau in AD.<sup>30–33</sup> We examined whether these putative kinases were also involved in the phosphorylation of tau in skeletal muscle, and whether modulating  $A\beta$ 42 levels in the MCK-APP/PS1 mice altered their activation state. The steady-state levels of total JNK, p38-MAPK, cdk5, and GSK-3 $\beta$  were not significantly altered among the transgenic mice at the ages tested (Figure 5, A and B). We first examined the activation/inactivation states of these kinases by measuring the phosphorylation profile of each kinase at specific amino acid residues. JNK and p38-MAPK are activated when phosphorylated at threonine 183 and tyrosine 185 or threonine 180 and tyrosine 182, respectively,<sup>34,35</sup> whereas phosphorylation at serine 9 in GSK-3 $\beta$  is considered to cause inactivation of its kinase activity.<sup>36,37</sup> At 6 months of age, we found lower levels of phosphorylated GSK-3 $\beta$  in the MCK-APP/PS1 mice (Figure 5A), and the reduction was significantly different from the other three groups ( $P < 0.01$ ). At 14 months of age, a marked reduction of phosphorylated GSK-3 $\beta$  was also observed only in the MCK-APP/PS1 mice (Figure 5B). Interestingly, at 14 months of age, the activation of p38-MAPK was also significantly increased as detected by the elevation of phosphorylated levels in both the MCK-APP and MCK-APP/PS1 mice (Figure 5B). Phosphorylated JNK levels were slightly decreased only in MCK-APP mice, whereas the levels in MCK-APP/PS1 mice were comparable to those in the non-Tg or PS1-KI mice (Figure 5B).

To further assess the involvement of these kinases in tau phosphorylation in the skeletal muscle of the MCK-APP/PS1 mice, we examined the association of these kinases with tau in skeletal muscle. We first immunoprecipitated proteins using the phospho-tau-specific antibody AT8 and determined which kinases were physically associated with phosphorylated tau in skeletal muscle. Markedly higher levels of cdk5 were detected in 6-month-old MCK-APP/PS1 mice, whereas higher levels of GSK-3 $\beta$  were found at 14 months (Figure 6A). Although increased activation of p38-MAPK was initially observed at 14 months, p38-MAPK as well as JNK were not co-immunoprecipitated with phosphorylated tau (data not shown), indicating that both p38-MAPK and JNK may be

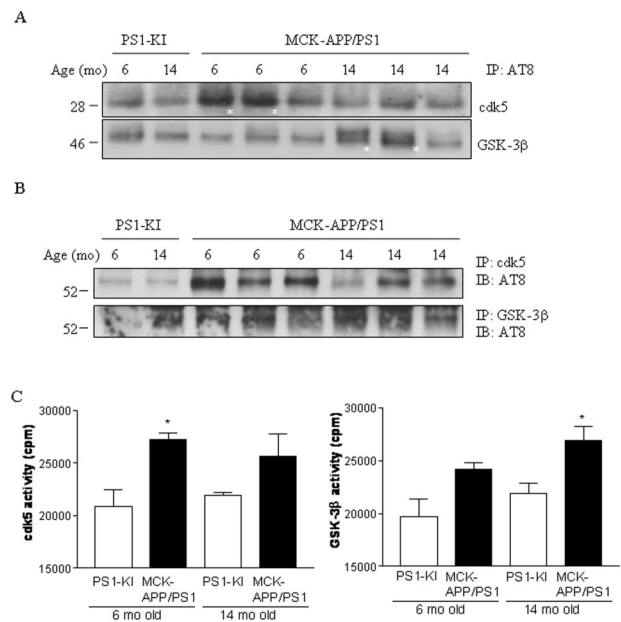


**Figure 6.** GSK-3 $\beta$  and cdk5 are activated and associated with phosphorylated tau in skeletal muscle from the MCK-APP/PS1 mice. **A:** Immunoblotting of cdk5 and GSK-3 $\beta$  after immunoprecipitation with antibody AT8 in skeletal muscle of 6- and 14-month-old PS1-KI or MCK-APP/PS1 mice. **Asterisk** indicates higher kinase levels associated with phosphorylated tau in the skeletal muscle. **B:** Reverse immunoprecipitation/immunoblot further confirms a physical association of cdk5 or GSK-3 $\beta$  with phosphorylated tau (recognized by AT8). **C:** Kinase activity of cdk5 (**left**) and GSK-3 $\beta$  (**right**) was measured from skeletal muscle of 6- and 14-month-old PS1-KI and MCK-APP/PS1 mice. Data represent mean  $\pm$  SEM from four mice per group. \* $P < 0.05$  compared to age-matched PS1-KI group.

less involved in tau phosphorylation in skeletal muscle. Moreover, immunoprecipitation with antibodies cdk5 or GSK-3 $\beta$  followed by immunoblotting with a tau antibody further confirmed the involvement of cdk5 and GSK-3 $\beta$  in tau phosphorylation in skeletal muscle of MCK-APP/PS1 mice (Figure 6B).

To further verify the activation states of cdk5 and GSK-3 $\beta$ , we measured the activity of these kinases. GSK-3 $\beta$  activity in skeletal muscle from the MCK-APP/PS1 mice was significantly higher at 14 months of age ( $P < 0.05$ ), whereas cdk5 activity was increased in the MCK-APP/PS1 mice at 6 months of age (Figure 6C). Although it was not significant, the GSK-3 $\beta$  activity at 6 months in the MCK-APP/PS1 was higher than PS1-KI mice, and it partially correlates with the reduction of phospho-GSK-3 $\beta$  levels (Figures 5A and 6C). Taken together, our results suggest that both GSK-3 $\beta$  and cdk5 are likely to be the primary kinases involved in the phosphorylation of tau in skeletal muscle of MCK-APP/PS1 mice, and that JNK and p38-MAPK are not likely to play a major role.

### Motor Impairment Associates with the Levels of $A\beta$ 42 in Skeletal Muscle

To assess the effect of the PS1 mutation and the subsequent enhancement of  $A\beta$ 42 levels on another function, we directly compared the performance of the double transgenic mice to controls using the acceler-

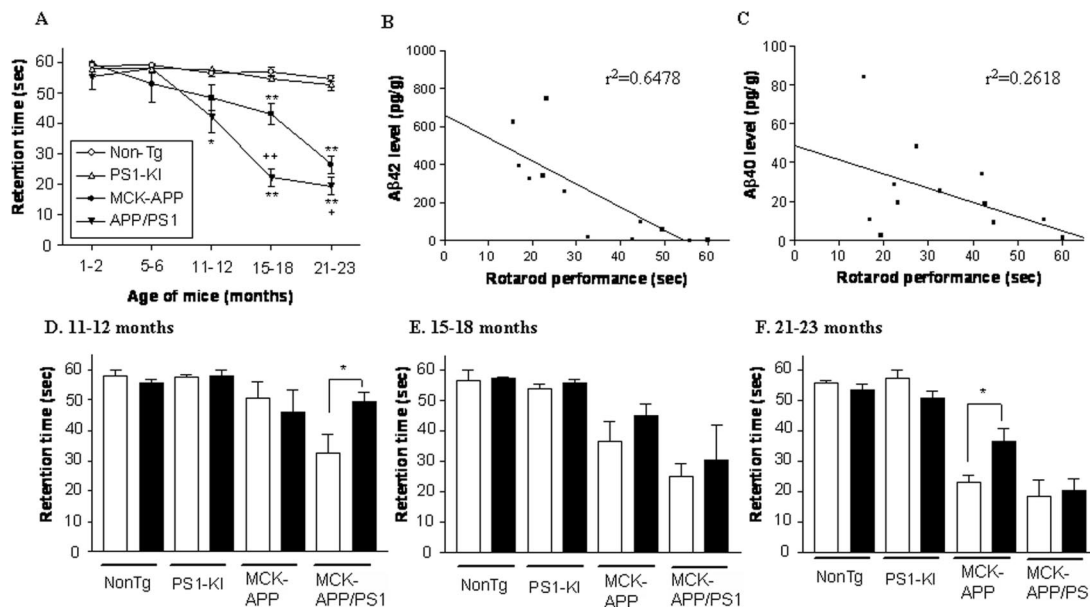


**Figure 7.** Augmenting Aβ42 exacerbates motor performance of the MCK-APP/PS1 mice. **A:** Age-dependent reduction of motor performance in both the MCK-APP and MCK-APP/PS1 mice. \* $P < 0.05$  or \*\* $P < 0.01$  as compared with non-Tg or PS1-KI. + $P < 0.05$  or ++ $P < 0.01$  as compared between MCK-APP and MCK-APP/PS1 mice. **B and C:** Correlation between accumulation of Aβ42 (**B**) or Aβ40 (**C**) in skeletal muscle and motor performance in MCK-APP/PS1 mice. The x-axis represents rotarod performance, and y axis represents Aβ levels in skeletal muscle. **D–F:** Sex difference in motor performance was analyzed at age 11 to 12 months (**D**), 15 to 18 months (**E**), and 21 to 23 months (**F**). Open and filled bars represent males and females, respectively. For all experiments, numbers of mice were used in each group:  $n = 4$  to 7 for 1 to 2 months,  $n = 4$  to 5 for 5 to 6 months,  $n = 8$  (four males and four females) for 11 to 12 months,  $n = 8$  to 13 (four to six males and four to seven females) for 15 to 18 months, and  $n = 8$  to 15 (four to six males and four to nine females) for 21 to 23 months. \* $P < 0.05$  compared between male and female.

ating rotarod. The motor performance of non-Tg, PS1-KI, MCK-APP, and double transgenic MCK-APP/PS1 mice was evaluated as a function of age. Five age groups were tested: 1 to 2, 5 to 6, 11 to 12, 15 to 18, and 21 to 23 months. Whereas the MCK-APP mice did not show impairments in motor performance until age 15 to 18 months, the MCK-APP/PS1 mice showed significant ( $P < 0.05$ ) impairment by 11 to 12 months of age (Figure 7A). Thus, augmenting Aβ42 levels in skeletal muscle shifted the onset age of impairment by several months. The disparity in motor performance was most notable between the two groups at 15 to 18 months of age, as the MCK-APP/PS1 mice were severely impaired compared to the single MCK-APP mice. By 21 to 23 months, the MCK-APP mice performed as poorly as the MCK-APP/PS1 mice. Both non-Tg and PS1-KI did not exhibit any significant reduction in motor performance at any of the ages tested. The impaired motor performance observed in the MCK-APP/PS1 mice strongly correlated with the buildup of Aβ42 in skeletal muscle ( $r^2 = 0.6478$ ; Figure 7B), whereas it was correlated in lesser degree with Aβ40 ( $r^2 = 0.2618$ ; Figure 7C), providing corroborating evidence for a pathogenic role for Aβ42 in muscle degeneration. In summary, we demonstrate that introduction of the mutant *PS1*<sub>M146V</sub> allele specifically increased the formation of Aβ42 and exacerbated the IBM-like phenotype.

Because there is a strong male predominance in IBM, we next evaluated male and female mice to determine whether there was a difference in performance between the sexes. Notably, we find that 11- to 12-month-old male

MCK-APP/PS1 mice performed significantly ( $P < 0.05$ ) poorer on the accelerating rotarod compared to age-matched female mice (Figure 7D). This disparity in motor performance was most apparent at this time point and diminished with age (Figure 7, E and F). Likewise, the male MCK-APP single transgenic mice were more severely impaired than the female counterparts at age 21 to 23 months (Figure 7F). Because the MCK-APP mice display less pathological features of IBM than the MCK-APP/PS1 mice, longer times are likely required for impairments to manifest in motor performance. In sum, we show that the phenotype of the MCK-APP and MCK-APP/PS1 mice correlates with the level of Aβ42 in skeletal muscle, with the higher Aβ42 levels in the MCK-APP/PS1 accelerating and exacerbating the phenotype relative to the MCK-APP mice.

## Discussion

The accumulation of Aβ within skeletal muscle fibers is one of the hallmark pathological features of IBM. Abnormal accumulation of Aβ-containing inclusions are present in skeletal muscle of IBM patients, and these inclusion bodies are found in nearly 100% of vacuolated muscle fibers.<sup>9,38</sup> Notably, these abnormal muscle fibers also accumulate presenilin-1,<sup>39</sup> which is considered to be the catalytic subunit of γ-secretase, suggesting that dysregulation of APP processing is involved in the disease onset and/or progression. However, it remains to be determined whether this buildup of Aβ is an epiphenomenon/consequence of the dis-

ease process or whether it plays a more direct role in contributing to the degenerative phenotype. Discriminating between these two possibilities is not readily feasible by analyzing histopathological muscle samples from affected human patients. Likewise, *in vivo* imaging methods have not yet reached the required point of sensitivity to address this question in living patients afflicted with the disease.

One means to better evaluate the role of A $\beta$  in the pathogenesis of skeletal muscle disorders such as IBM is to use animal models. Because IBM is a chronic, age-related disorder like AD, we used an aggressive genetic approach to generate a mouse model that exhibits relevant pathology by overexpressing APP selectively in skeletal muscle. Notably, there is evidence that APP mRNA levels are selectively enhanced in human IBM samples,<sup>40</sup> thereby providing physiological justification for the overexpression of this protein in transgenic mice. We previously generated a transgenic model of this myopathy by selectively targeting the precursor of A $\beta$  (APP) to skeletal muscle fibers with the use of the MCK promoter.<sup>21</sup> These MCK-APP transgenic mice develop IBM-like pathology as well as an age-dependent motor impairment. The mice also predominantly produce the less amyloidogenic A $\beta$ 40 isoform. However, it is well established, at least for brain amyloid disorders like AD, that the longer A $\beta$ 42 species is far more pathogenic. Consequently, here we used a genetic approach to modulate  $\gamma$ -secretase activity to favor production of A $\beta$ 42, by introducing a mutant PS1<sub>M146V</sub> allele into the MCK-APP transgenic mice. This goal was readily achieved by crossing the MCK-APP mice to the PS1<sub>M146V</sub> knock-in mice. These double transgenic MCK-APP/PS1 mice produce significantly higher levels of the A $\beta$ 42 peptide in skeletal muscle relative to single, parental line. Likewise, the A $\beta$ 42/40 ratio is also significantly higher. Through analysis of the single and double transgenic lines developed here, we were able to determine whether A $\beta$ 40 or A $\beta$ 42 plays a more detrimental role in skeletal muscle. As shown in the result, higher levels of A $\beta$ 42 in skeletal muscle seem to exacerbate the phenotype, leading to the earlier manifestation of the IBM-like histopathological features and the motor impairment relative to the parental line.

Because the phenotype is exacerbated by the increased levels of A $\beta$ 42, it provides strong *in vivo* evidence that this peptide likely plays a pathogenic role in IBM, and likely not to be simply a marker or epiphenomenon. It is critical to emphasize that the introduction of the mutant PS1 allele did not enhance or alter the cellular profile of APP expression, thus the accelerated phenotype is solely due to the modulation of APP processing and elevated levels of A $\beta$ 42. Higher A $\beta$ 42 levels can have detrimental consequences for the AD brain, and our present findings demonstrate a similar finding is also true for skeletal muscle. Although our data show that augmenting A $\beta$ 42 levels in muscle accelerates the pathology and motor deficits, it does not address the mechanism by which high levels of the intracellular A $\beta$ 42 peptide cause disease.

Several pathogenic mechanisms induced by mismetabolism of APP have been proposed, and one or more of

these mechanisms may underlie the exacerbated phenotype we described here. Christensen and colleagues<sup>41</sup> recently found a marked elevation of basal calcium stores in cultured myogenic cells overexpressing A $\beta$ 42, and they also found that the sensitivity of ryanodine receptors to caffeine was significantly increased in the presence of A $\beta$ 42 in these cells. Although the exact consequences of altering calcium levels in skeletal muscle remain to be elucidated, their results indicate that calcium dyshomeostasis may be one of the pathogenic causes of IBM, and further work will be required to determine whether a similar alteration occurs in the transgenic mice.

Another potential mechanism that may be affected is the proteasome. APP/A $\beta$ -mediated proteasome inhibition was recently reported by Fratta and colleagues.<sup>42</sup> They studied skeletal muscles from sporadic IBM patients and found that proteasome subunit (20S $\alpha$ ) was co-localized with APP/A $\beta$ , and its proteolytic activity was significantly reduced compared to healthy skeletal muscles. Furthermore, cultured muscle fibers overexpressing APP showed a marked reduction of proteasome activity, and a proteasome inhibitor, epoxomicin, increased the formation of inclusion bodies.<sup>42</sup> These data strongly suggest that pathological features of IBM including A $\beta$  and hyperphosphorylated tau-containing inclusion bodies and vacuole formation may be partially due to proteasome inhibition caused by the abnormal buildup of A $\beta$  in muscle fibers.

Interestingly, the MCK-APP/PS1 mice showed a marked elevation of phosphorylated tau in skeletal muscle in an age-dependent manner. Increased levels of AT8-positive tau correlated well with production of intramuscular A $\beta$  levels and were likely mediated by the differential activation of cdk5 and GSK-3 $\beta$ . Our current data strongly suggest that cellular mechanisms of tau pathology in this IBM model are similar to those in AD because both cdk5 and GSK-3 $\beta$  play a critical role in the pathogenesis of neurofibrillary tangles.<sup>43–45</sup> In IBM-afflicted skeletal muscle, higher levels of cdk5 have been observed, and it is co-localized with phosphorylated tau.<sup>46,47</sup>

Although the molecular basis that triggers the onset of IBM remains unknown, the findings of this study indicate that mechanisms underlying IBM may be similar to those in AD. In both disorders, A $\beta$  seems to play a pivotal pathogenic role. Of course, the ultimate demonstration that A $\beta$  is critically involved in the pathogenesis of IBM will await clinical trials. Given the remarkable pathobiochemical similarities between AD and IBM, it will be interesting to determine whether A $\beta$ -directed therapies that are in preclinical or clinical development for AD, such as BACE or  $\gamma$ -secretase inhibitors or A $\beta$  immunotherapy have therapeutically beneficial results for IBM patients as well.

## References

1. Tawil R, Griggs RC: Inclusion body myositis. *Curr Opin Rheumatol* 2002, 14:653–657
2. Beyenburg S, Zierz S, Jerusalem F: Inclusion body myositis: clinical

- and histopathological features of 36 patients. *Clin Invest* 1993, 71:351–361
3. Dalakas MC: Clinical, immunopathologic, and therapeutic considerations of inflammatory myopathies. *Clin Neuropharmacol* 1992, 15:327–351
  4. Vasconcelos OM, Raju R, Dalakas MC: GNE mutations in an American family with quadriceps-sparing IBM and lack of mutations in s-IBM. *Neurology* 2002, 59:1776–1779
  5. Eisenberg I, Grabov-Nardini G, Hochner H, Korner M, Sadeh M, Bertorini T, Bushby K, Castellani C, Felice K, Mendell J, Merlini L, Shilling C, Wirguin I, Argov Z, Mitrani-Rosenbaum S: Mutations spectrum of GNE in hereditary inclusion body myopathy sparing the quadriceps. *Hum Mutat* 2003, 21:99
  6. Maurage CA, Bussiere T, Sergeant N, Ghestem A, Figarella-Branger D, Ruchoux MM, Pellissier JF, Delacourte A: Tau aggregates are abnormally phosphorylated in inclusion body myositis and have an immunoelectrophoretic profile distinct from other tauopathies. *Neuropathol Appl Neurobiol* 2004, 30:624–634
  7. Lotz BP, Engel AG, Nishino H, Stevens JC, Litchy WJ: Inclusion body myositis. Observations in 40 patients. *Brain* 1989, 112:727–747
  8. Mendell JR, Sahenk Z, Gales T, Paul L: Amyloid filaments in inclusion body myositis. Novel findings provide insight into nature of filaments. *Arch Neurol* 1991, 48:1229–1234
  9. Askanas V, Engel WK, Alvarez RB: Enhanced detection of Congo-red-positive amyloid deposits in muscle fibers of inclusion body myositis and brain of Alzheimer's disease using fluorescence technique. *Neurology* 1993, 43:1265–1267
  10. Mirabella M, Alvarez RB, Bilak M, Engel WK, Askanas V: Difference in expression of phosphorylated tau epitopes between sporadic inclusion-body myositis and hereditary inclusion-body myopathies. *J Neuropathol Exp Neurol* 1996, 55:774–786
  11. Yoshida T, Ohno-Matsui K, Ichinose S, Sato T, Iwata N, Saido TC, Hisatomi T, Mochizuki M, Morita I: The potential role of amyloid beta in the pathogenesis of age-related macular degeneration. *J Clin Invest* 2005, 115:2793–2800
  12. Tseng BP, Kitazawa M, LaFerla FM: Amyloid beta-peptide: the inside story. *Curr Alzheimer Res* 2004, 1:231–239
  13. Billings LM, Oddo S, Green KN, McGaugh JL, Laferla FM: Intraneuronal Abeta causes the onset of early Alzheimer's disease-related cognitive deficits in transgenic mice. *Neuron* 2005, 45:675–688
  14. Oddo S, Caccamo A, Shepherd JD, Murphy MP, Golde TE, Kaye R, Metherate R, Mattson MP, Akbari Y, LaFerla FM: Triple-transgenic model of Alzheimer's disease with plaques and tangles: intracellular Abeta and synaptic dysfunction. *Neuron* 2003, 39:409–421
  15. McLean CA, Cherny RA, Fraser FW, Fuller SJ, Smith MJ, Beyreuther K, Bush AI, Masters CL: Soluble pool of Abeta amyloid as a determinant of severity of neurodegeneration in Alzheimer's disease. *Ann Neurol* 1999, 46:860–866
  16. Lue LF, Kuo YM, Roher AE, Brachova L, Shen Y, Sue L, Beach T, Kurth JH, Rydel RE, Rogers J: Soluble amyloid beta peptide concentration as a predictor of synaptic change in Alzheimer's disease. *Am J Pathol* 1999, 155:853–862
  17. Gong Y, Chang L, Viola KL, Lacor PN, Lambert MP, Finch CE, Krafft GA, Klein WL: Alzheimer's disease-affected brain: presence of oligomeric A beta ligands (ADDLs) suggests a molecular basis for reversible memory loss. *Proc Natl Acad Sci USA* 2003, 100:10417–10422
  18. Kaye R, Head E, Thompson JL, McIntire TM, Milton SC, Cotman CW, Glabe CG: Common structure of soluble amyloid oligomers implies common mechanism of pathogenesis. *Science* 2003, 300:486–489
  19. Walsh DM, Tseng BP, Rydel RE, Podlisny MB, Selkoe DJ: The oligomerization of amyloid beta-protein begins intracellularly in cells derived from human brain. *Biochemistry* 2000, 39:10831–10839
  20. Oddo S, Caccamo A, Tran L, Lambert MP, Glabe CG, Klein WL, Laferla FM: Temporal profile of amyloid-beta (Abeta) oligomerization in an in vivo model of Alzheimer disease: a link between Abeta and tau pathology. *J Biol Chem* 2006, 281:1599–1604
  21. Sugarman MC, Yamasaki TR, Oddo S, Echegoyen JC, Murphy MP, Golde TE, Jannatipour M, Leissring MA, LaFerla FM: Inclusion body myositis-like phenotype induced by transgenic overexpression of beta APP in skeletal muscle. *Proc Natl Acad Sci USA* 2002, 99:6334–6339
  22. Duff K, Eckman C, Zehr C, Yu X, Prada CM, Perez-tur J, Hutton M, Buee L, Harigaya Y, Yager D, Morgan D, Gordon MN, Holcomb L, Refolo L, Zenk B, Hardy J, Younkin S: Increased amyloid-beta42(43) in brains of mice expressing mutant presenilin 1. *Nature* 1996, 383:710–713
  23. Scheuner D, Eckman C, Jensen M, Song X, Citron M, Suzuki N, Bird TD, Hardy J, Hutton M, Kukull W, Larson E, Levy-Lahad E, Viitanen M, Peskind E, Poorkaj P, Schellenberg G, Tanzi R, Wasco W, Lannfelt L, Selkoe D, Younkin S: Secreted amyloid beta-protein similar to that in the senile plaques of Alzheimer's disease is increased in vivo by the presenilin 1 and 2 and APP mutations linked to familial Alzheimer's disease. *Nat Med* 1996, 2:864–870
  24. Borchelt DR, Thinakaran G, Eckman CB, Lee MK, Davenport F, Ratovitsky T, Prada CM, Kim G, Seekins S, Yager D, Slunt HH, Wang R, Seeger M, Levey AI, Gandy SE, Copeland NG, Jenkins NA, Price DL, Younkin SG, Sisodia SS: Familial Alzheimer's disease-linked presenilin 1 variants elevate Abeta1-42/1-40 ratio in vitro and in vivo. *Neuron* 1996, 17:1005–1013
  25. Citron M, Westaway D, Xia W, Carlson G, Diehl T, Levesque G, Johnson-Wood K, Lee M, Seubert P, Davis A, Kholodenko D, Motter R, Sherrington R, Perry B, Yao H, Strome R, Lieberburg I, Rommens J, Kim S, Schenk D, Fraser P, St. George Hyslop P, Selkoe DJ: Mutant presenilins of Alzheimer's disease increase production of 42-residue amyloid beta-protein in both transfected cells and transgenic mice. *Nat Med* 1997, 3:67–72
  26. Guo Q, Fu W, Sopher BL, Miller MW, Ware CB, Martin GM, Mattson MP: Increased vulnerability of hippocampal neurons to excitotoxic necrosis in presenilin-1 mutant knock-in mice. *Nat Med* 1999, 5:101–106
  27. Kitazawa M, Oddo S, Yamasaki TR, Green KN, LaFerla FM: Lipopolysaccharide-induced inflammation exacerbates tau pathology by a cyclin-dependent kinase 5-mediated pathway in a transgenic model of Alzheimer's disease. *J Neurosci* 2005, 25:8843–8853
  28. Sugarman MC, Kitazawa M, Baker M, Caiozzo VJ, Querfurth HW, Laferla FM: Pathogenic accumulation of APP in fast twitch muscle of IBM patients and a transgenic model. *Neurobiol Aging* 2006, 27:423–432
  29. Adams JH, DuChen LW: *Greenfield's Neuropathology*. New York, Oxford University Press, 1992
  30. Atzori C, Ghetti B, Piva R, Srinivasan AN, Zolo P, Delisle MB, Mirra SS, Ghiglieri A: Activation of the JNK/p38 pathway occurs in diseases characterized by tau protein pathology and is related to tau phosphorylation but not to apoptosis. *J Neuropathol Exp Neurol* 2001, 60:1190–1197
  31. Savage MJ, Lin YG, Ciallella JR, Flood DG, Scott RW: Activation of c-Jun N-terminal kinase and p38 in an Alzheimer's disease model is associated with amyloid deposition. *J Neurosci* 2002, 22:3376–3385
  32. Sun W, Qureshi HY, Cafferty PW, Sobue K, Agarwal-Mawal A, Neufeld KD, Paudel HK: Glycogen synthase kinase-3beta is complexed with tau protein in brain microtubules. *J Biol Chem* 2002, 277:11933–11940
  33. Liu SJ, Zhang AH, Li HL, Wang Q, Deng HM, Netzer WJ, Xu H, Wang JZ: Overactivation of glycogen synthase kinase-3 by inhibition of phosphoinositol-3 kinase and protein kinase C leads to hyperphosphorylation of tau and impairment of spatial memory. *J Neurochem* 2003, 87:1333–1344
  34. Raingeaud J, Gupta S, Rogers JS, Dickens M, Han J, Ulevitch RJ, Davis RJ: Pro-inflammatory cytokines and environmental stress cause p38 mitogen-activated protein kinase activation by dual phosphorylation on tyrosine and threonine. *J Biol Chem* 1995, 270:7420–7426
  35. Lawler S, Fleming Y, Goedert M, Cohen P: Synergistic activation of SAPK1/JNK1 by two MAP kinase kinases in vitro. *Curr Biol* 1998, 8:1387–1390
  36. Cohen P, Frame S: The renaissance of GSK3. *Nat Rev Mol Cell Biol* 2001, 2:769–776
  37. Shaw M, Cohen P, Alessi DR: Further evidence that the inhibition of glycogen synthase kinase-3beta by IGF-1 is mediated by PDK1/PKB-induced phosphorylation of Ser-9 and not by dephosphorylation of Tyr-216. *FEBS Lett* 1997, 416:307–311
  38. Askanas V, Alvarez RB, Engel WK: Beta-amyloid precursor epitopes in muscle fibers of inclusion body myositis. *Ann Neurol* 1993, 34:551–560
  39. Askanas V, Engel WK, Yang CC, Alvarez RB, Lee VM, Wisniewski T: Light and electron microscopic immunolocalization of presenilin 1 in abnormal muscle fibers of patients with sporadic inclusion-body myositis and autosomal-recessive inclusion-body myopathy. *Am J Pathol* 1998, 152:889–895

40. Sarkozi E, Askanas V, Johnson SA, Engel WK, Alvarez RB: Beta-amyloid precursor protein mRNA is increased in inclusion-body myositis muscle. *Neuroreport* 1993, 4:815–818
41. Christensen RA, Shtifman A, Allen PD, Lopez JR, Querfurth HW: Calcium dyshomeostasis in beta-amyloid and tau-bearing skeletal myotubes. *J Biol Chem* 2004, 279:53524–53532
42. Fratta P, Engel WK, McFerrin J, Davies KJ, Lin SW, Askanas V: Proteasome inhibition and aggresome formation in sporadic inclusion-body myositis and in amyloid-beta precursor protein-overexpressing cultured human muscle fibers. *Am J Pathol* 2005, 167:517–526
43. Sengupta A, Wu Q, Grundke-Iqbal I, Iqbal K, Singh TJ: Potentiation of GSK-3-catalyzed Alzheimer-like phosphorylation of human tau by cdk5. *Mol Cell Biochem* 1997, 167:99–105
44. Augustinack JC, Sanders JL, Tsai LH, Hyman BT: Colocalization and fluorescence resonance energy transfer between cdk5 and AT8 suggests a close association in pre-neurofibrillary tangles and neurofibrillary tangles. *J Neuropathol Exp Neurol* 2002, 61:557–564
45. Pei JJ, Grundke-Iqbal I, Iqbal K, Bogdanovic N, Winblad B, Cowburn RF: Accumulation of cyclin-dependent kinase 5 (cdk5) in neurons with early stages of Alzheimer's disease neurofibrillary degeneration. *Brain Res* 1998, 797:267–277
46. Nakano S, Akiguchi I, Nakamura S, Sato H, Kawashima S, Kimura J: Aberrant expression of cyclin-dependent kinase 5 in inclusion body myositis. *Neurology* 1999, 53:1671–1676
47. Wilczynski GM, Engel WK, Askanas V: Cyclin-dependent kinase 5 colocalizes with phosphorylated tau in human inclusion-body myositis paired-helical filaments and may play a role in tau phosphorylation. *Neurosci Lett* 2000, 293:33–36